

# Punctuated vortex coalescence and discrete scale invariance in two-dimensional turbulence

Anders Johansen<sup>1</sup>, Didier Sornette<sup>1,2,3</sup>, and Adam Espe Hansen<sup>4,5</sup>

<sup>1</sup> Institute of Geophysics and Planetary Physics  
University of California, Los Angeles, California 90095

<sup>2</sup> Department of Earth and Space Science  
University of California, Los Angeles, California 90095

<sup>3</sup> Laboratoire de Physique de la Matière Condensée  
CNRS UMR6622 and Université des Sciences, B.P. 70, Parc Valrose  
06108 Nice Cedex 2, France

<sup>4</sup> Niels Bohr Institute, Ørsted Laboratory,  
Universitetsparken, 2100 Kbh. Ø, Denmark

<sup>5</sup> Laboratoire de Physique Statistique, École Normale Supérieure  
24 rue Lhomond, 75231 Paris, France

April 26, 2024

## Abstract

We present experimental evidence and theoretical arguments showing that the time-evolution of freely decaying 2-d turbulence is governed by a *discrete* time scale invariance rather than a continuous time scale invariance. Physically, this reflects that the time-evolution of the merging of vortices is not smooth but punctuated, leading to a preferred scale factor and as a consequence to log-periodic oscillations. From a thorough analysis of freely decaying 2-d turbulence experiments, we show that the number of vortices, their radius and separation display log-periodic oscillations as a function of time with an average log-frequency of  $\approx 4 - 5$  corresponding to a preferred scaling ratio of  $\approx 1.2 - 1.3$ .

# 1 Introduction

Hydrodynamical turbulence is one of the major remaining challenges in the physical sciences. It provides a fascinating phenomenology with both simple universal scaling laws and complex system specific features. Two-dimensional turbulence is of special interest, both for its applications in astrophysics and geophysics and its theoretical properties. It is also more amenable to detailed experimental, numerical and theoretical studies. Its main characteristic property is the formation of and interaction between coherent structures or vortices.

Kolmogorov first proposed his energy cascade model which was later refined by many authors to account for intermittency effects (see for instance [1]). It remains to be assessed to what extent this class of statistical phenomenological models is physically correct and whether the the cascade picture can be taken to represent real physical processes that occur genuinely in fluids.

2-d turbulence is distinct from 3-d turbulence by the conservation of vorticity along fluid particle paths, when ignoring viscosity and forcing (there are no vortex-stretching term in the 2-d equations). An inverse energy cascade was conjectured by Kraichnan [2] and has since been largely confirmed by simulations and experiments (see for instance Ref.[1] and references therein). This inverse cascade does not appear to be characterised by the presence of strong coherent vortices. Similarly, if the direct cascade exists in 3-d turbulence, vortex filaments are also rare events but, according to the so-called hierarchical structure model [3], they nevertheless play an important role. These coherent structures are the most singular, the most intermittent, and the rarest events in a turbulent medium; these structures are also the most sensitive structures depending on the environment. According to this theory, “softer” fluctuations are organised statistically into a hierarchy which satisfies universal statistical symmetry with scaling exponents controlled by the nature of these most singular structures.

Returning to the 2-d inverse energy cascade, the coherent vortices are clearly identified at the forcing scale, comparable to the system size. Their statistical properties suggest that the cascade is driven by a clustering mechanism involving vortices of the same sign [4], in contrast to the sequence of merging events producing larger and larger vortices occurring in freely decaying 2-d turbulence which we analyse below. In the inverse cascade, the energy is thus transported to larger scales by an aggregation of vortices of the same sign while no apparent fusion is present, in contrast to freely decaying 2-d turbulence. In addition, the inverse cascade appears non-intermittent with regular Gaussian statistical properties of the velocity increments. The generalisation of our finding obtained in a situation of vortex merging to forced 2-d turbulence where vortices do not merge but aggregate and its relevance to the energy cascade (inverse in 2-d and direct in 3-d) are thus conjectural and remain to be tested directly.

Here, we identify a novel signature of 2-d freely decaying turbulent flows suggesting that vortex merging occur via a cascade process with a discrete hierarchy of sizes. We document log-periodic oscillations, which are the hallmarks of a discrete hierarchical structure with a preferred scaling ratio, in the time evolution of the number of vortices, their radius and separation.

The theory of log-periodicity (and its associated complex exponents) has advanced significantly [5] in the last few years. Log-periodicity reflects a discrete scale invariance, i.e., the fact that dilational symmetry occurs only under magnification under special factors, which are arbitrary powers  $\lambda^n$  of a preferred scaling ratio  $\lambda$ . Log-periodicity has been studied in the eighties in relation to various problems of physics embedded in discrete hierarchical systems. In the context of turbulence, shell models construct explicitly a discrete scale invariant set of equations whose solutions are marred by unwanted log-periodicities. Only recently has it been realized that discrete scale invariance and its associated complex exponents may appear “spontaneously” in Euclidean systems, i.e., without the need for a pre-existing hierarchy (see [5] for references and

discussion of Laplacian growth models, rupture in heterogeneous systems, earthquakes, animals, financial crashes among many other systems). In addition, general field theoretical arguments [6] indicate that complex exponents are to be expected generically for out-of-equilibrium and quenched disordered systems.

The paper is organised as follows. In section 2, we discuss the plausibility of log-periodicity in turbulence from the vantage of three theoretical arguments based on similarity analysis, mean field theory and the aggregation analogy. In section 3 we describe our statistical tools, in particular the Lomb periodogram technique and its performance on synthetic tests with a detailed discussion of the role of noise and the problem of averaging. These considerations concerning detection of log-periodic signals are offered to point-out important pit-falls, which might explain why such signals have not previously been reported. The experimental set-up, main experimental results and our analysis of the experimental data are presented in section 4 while section 5 concludes.

## 2 Theory

There is no established theory on 2-d freely decaying turbulence. All available approaches exhibit some weaknesses or incompatibilities with experiments. Here we discuss three of the main theoretical approaches only to suggest that log-periodicity is not unreasonable from a theoretical view point.

### 2.1 Dimensional analysis and Similarity of the third kind

Scaling laws are tools which can be used to quantify the complexity of turbulent flows. Well-known examples include the Kolmogorov energy-cascade from large scales to smaller scales in 3-d turbulence and from small scales to larger scales in forced 2-d turbulence [1], as already mentioned.

For the decaying 2-d case, the flow carries coherent vortices [7]. Let us assume that the number of vortices also obeys a scaling law. Using the  $\Pi$  theorem of dimensional analysis [8], which states that the laws of physics must be such as to be expressed using only dimensionless variables, it can be written as

$$n(t) \sim \frac{1}{Et^2} F(Re, \frac{t}{t_L}, \frac{t}{\tau}, \dots) . \quad (1)$$

Here  $E$  is the kinetic energy per area,  $Re$  is the Reynolds number inversely proportional to the viscosity  $\nu$ ,  $t_L = L/\langle v \rangle$  is the typical time scale for a vortex to move over the system size  $L$  and  $\tau = \langle R \rangle / \langle v \rangle$  is the typical time for a vortex to move over a distance comparable to its typical radius. That the first term of the r.h.s. is inversely proportional to  $Et^2$  stems from the fact that  $E$  is proportional to the inverse of a time-squared.

The simplest assumption [9] is that the function  $F$  goes to a constant when the viscosity  $\nu \rightarrow 0$ , leading to the prediction  $n(t) \sim \frac{1}{t^2}$ . This corresponds to the so-called complete similarity of the first kind [8] with respect to the variables  $Re$ ,  $t/t_L$  and  $t/\tau$ .

The existence of a finite limit of  $F$  was first questioned by L.D. Landau and A.M. Obukhov in the context of fully developed turbulence in 3-d, on the basis of the existence of intermittency – large fluctuations of the energy dissipation rate about its mean value. Following the same argument and Barenblatt’s classification leads to the possibility of an *incomplete similarity* in the variables  $t/t_L$  and  $t/\tau$ . This would require the absence of a finite limit for  $F(Re, \frac{t}{t_L}, \frac{t}{\tau}, \dots)$  as  $t/t_L \rightarrow 0$  or as  $t/\tau \rightarrow \infty$ , and leads in the simplest case to the form

$$n(t) \sim \frac{1}{Et^2} \left(\frac{t}{t_L}\right)^\alpha \left(\frac{t}{\tau}\right)^\beta \sim \frac{1}{t^\xi} , \quad \text{with } \xi \equiv 2 - \alpha - \beta , \quad (2)$$

where  $\alpha$  and  $\beta$  are intermittency exponents. If  $\alpha$  and  $\beta$  are real, this corresponds to a similarity of the second kind [8].

Incomplete self-similarity [10, 11] may stem from a possible dependence of the exponents on  $Re$ . Dubrulle [12] (see also [13]) has proposed to call the case where  $\alpha$  and/or  $\beta$  is complex, leading to

$$n(t) \sim \frac{1}{t^{\xi_R}} \cos[\xi_I \ln t + \psi] , \quad (3)$$

a similarity of the third kind, characterised by the absence of limit for  $F(Re, \frac{t}{t_L}, \frac{t}{\tau}, \dots)$  and accelerated (log-periodic) oscillations.

To our knowledge, Novikov has been the first to point out in 1966 that structure functions in 3-d turbulence should contain log-periodic oscillations [14]. His argument was that if an unstable eddy in a turbulent flow typically breaks up into two or three smaller eddies, but not into 10 or 20 eddies, then one can suspect the existence of a preferred scale factor, hence the log-periodic oscillations. This view does not seem to be born out by direct observation of 3-d flows where vortex filaments are very rare events and the cascade seems to occur via a different mechanism. The dynamical occurrence of a discrete hierarchy of velocity fluctuation remains to be investigated. Notice however that our finding of a discrete hierarchy of merging events in freely decaying 2-d turbulence is in a sense reverse to Novikov's picture.

Log-periodic oscillations have been repeatedly observed in structure factors but do not seem to be stable and depend on the nature of the global geometry of the flow and recirculation [1, 15] as well as the analysing procedure. As to be discussed in section 3, the detection of log-periodic structures in data is a non-trivial task and is rather sensitive to the implementation of the analysis.

## 2.2 Mean field theory

At times sufficiently large so that the individual mean time between two collisions suffered by any one vortex is larger than the time needed for a typical vortex to move the distance of its typical diameter, we can use Trizac's mean field approach [16] based on dimensional analysis. The fundamental equation resulting from this analysis governs the time evolution of the vortex density  $n(t)$ :

$$\frac{dn}{dt} = -\xi \frac{n(t)}{t} . \quad (4)$$

It integration gives the usual power law solution

$$n(t) \sim t^{-\xi} , \quad (5)$$

where  $\xi$  is empirically found equal to  $0.72 \pm 0.03$  while theoretical arguments suggest  $\xi = 1$  [17, 18] or  $\xi = 0.8$  [16].

It is important to recognise that (4) represents an averaging over highly intermittent and "non-smooth" processes: most of the time, the dynamics of the freely decaying 2-d turbulence is dominated by the mutual advection of the vortices, while rare dissipative events of energetic vortex merging punctuate this dynamics. Thus, in reality, the time dynamics is not scale free as expression (4) would lead us to believe. There are rather well-defined instants at which the coalescence proceeds, corresponding to a discrete time evolution for the number of vortices, and the occurrence of these instants have to obey a scale invariance in time dilation in order to recover (4) on average.

Let us now go beyond this average description and attempt to describe this punctuated dynamics by introducing time scales in the simplest way such as to recover the continuous time scale invariance (CTSI) upon averaging: we hypothesise that the sudden coalescence can be

accounted for by breaking partially the CTSI captured by expression (4) into a weaker *discrete* time scale invariance (DTSI). Quantitatively, this amounts to replacing (4) by expressing  $dt$  as a discrete time step approximation with should also be scale invariant :

$$dt = \alpha t , \quad (6)$$

with  $\alpha$  a characteristic scale ratio. Then, (4) transforms into

$$\frac{n(t + \alpha t) - n(t)}{\alpha t} = -\xi \frac{n(t)}{t} ,$$

leading to

$$n(\lambda t) = (1 - (\lambda - 1)\xi) n(t) , \quad \text{where } \lambda \equiv 1 + \alpha . \quad (7)$$

Expression (7) is now a discrete scale invariant relation for  $n(t)$ . Its general solutions are power laws  $t^{-s_m}$  like (5), where the exponents  $s_m$  now depend on  $\alpha$  and can acquire an imaginary part. It is this imaginary part which is the signature of a discrete hierarchy of time scales reflected in log-periodic oscillations :

$$s_m = -\frac{\ln(1 - (\lambda - 1)\xi)}{\ln \lambda} + im \frac{2\pi}{\ln \lambda} , \quad (8)$$

where  $i = \sqrt{-1}$  and  $m$  is an integer. The real solution  $s_0$  recovers the value  $\xi$  in the limit  $\alpha \rightarrow 0, \lambda \rightarrow 1$ , where the discrete scale symmetry recovers the continuous scale symmetry.

We see that, for  $\lambda > 1, s_0 > \xi$ . As an example, take the experimentally determined value  $\xi = 0.72$ , which gives  $s_0 = 0.80$  for  $\lambda = 1.13$  and  $s_0 = 1.01$  for  $\lambda = 1.4$ . For  $\lambda = 1.2$ , we get  $s_0 = 0.85$ . This suggests an explanation for the difference between prediction from theory and experimental and numerical data: the measurements that assume CTSI underestimate the true value that is impregnated by the existence the punctuated dynamics leading to DTSI.

In this formalism, one can take into account the presence of fluctuations in the rate of vortex mergers by replacing (7) by

$$n(\lambda_1 t_0) = (1 - (\lambda_1 - 1)\xi_1) n(t_0) \quad (9)$$

$$n(\lambda_2 \lambda_1 t_0) = (1 - (\lambda_2 - 1)\xi_2) n(\lambda_1 t_0) \quad (10)$$

$$\dots \quad (11)$$

$$n\left(\prod_{i=1}^N \lambda_i t_0\right) = n(t_0) \prod_{i=1}^N (1 - (\lambda_i - 1)\xi_i) . \quad (12)$$

These equations describe the fact that the hierarchy of time scales at which the vortex mergers occur do not need to obey an exact hierarchy but can exhibit fluctuations. Looking for a power law behaviour  $n(t) \sim t^{-s}$ , we find that the *typical* value for  $s$  is given by [6]

$$s_m = -\frac{\langle \ln(1 - (\lambda - 1)\xi) \rangle}{\langle \ln \lambda \rangle} + im \frac{2\pi}{\langle \ln \lambda \rangle} , \quad (13)$$

where the averaging  $\langle \cdot \rangle$  is performed over the distributions of  $\lambda$  and  $\xi$ .

### 2.3 Linear theory of aggregation

Benzi et al. [19] and McWilliams [20] have noted the analogy between the vortex merging in turbulence and the kinetic theory of colloidal aggregation [21]. Starting from a population

$n_1(t = 0)$  of monomers, the kinetic equations of aggregation read

$$\frac{dn_1}{dt} = -n_1 \sum_{i=1}^{\infty} J_{1,i} n_i \quad (14)$$

$$\frac{dn_j}{dt} = \sum_{i=1}^{j-1} J_{i,i-j} n_i n_{j-i} - n_j \sum_{i=1}^{\infty} J_{i,j} n_i . \quad (15)$$

The first equation expresses that the population of monomers decreases by coalescence with all possible species. The second equation expresses the competition between the formation of a  $j$ -mer by coalescence of an  $i$ -mer and a  $j - i$ -mer and its destruction by coalescence with all possible species. The  $J_{i,j}$  express the rates at which these coagulation occur. When diffusion motion dominates, we have

$$J_{i,j} \sim (R_i + R_j)(D_i + D_j) , \quad (16)$$

where  $R_i$  (resp.  $D_i$ ) is the radius (resp. diffusion coefficient) of the  $i$ -mer. From Stokes law and Einstein's relationship,  $D \sim 1/R$  the kernel are homogeneous:  $J_{\lambda i, \lambda j} = J_{i,j}$ . In this case, the  $J_{i,j}$  can be taken constant and (15) reduces to

$$\frac{dn_1}{dt} = -An_1 n \quad (17)$$

$$\frac{dn}{dt} = \frac{A}{2} n_1^2 - \frac{1}{2} n^2 , \quad (18)$$

where  $n(t) = \sum_{i=1}^{\infty} n_i$  is the total population. It is then straightforward to check that  $n_1(t) \sim n(t) \sim 1/t$  at large  $t$ .

A fundamental physical ingredient in this approach is the quadratic pair-wise nature of the interactions described by the r.h.s. of the equations (15,18), which embodies the idea that coagulation is a stochastic process requiring the chancy collision of *two* particles that can come from arbitrary position in space. We argue quite reasonably that this is not the correct situation for vortex fusion in freely decaying 2-d turbulence due to the confinement that a 2-d space represents. Experiments (see for example figure 3 of Ref.[22]) show that, between two merging events, vortices move as in a flexible "cage" of neighbouring vortices. Thus, the relevant rate of fusion is not proportional to the square of the number of vortices but to the first power, since each vortex can only merge with those vortices at its perimeter that do not evolve significantly over long period of times. In other words, there is not an efficient mixing and hence the mean-field approximation underlying eq.s (15) and (18) breaks down.

As a consequence, we can write down a *linear* integro-differential coupled equation for the time evolution of the vortex populations, in close analogy to the scaling theory of linear fragmentation of Ref.[23, 24]. A remarkable feature of this approach is that the analysis can be carried out for arbitrary scaling kernels.

It is convenient to define the distribution  $\Phi(E, t)$  of vortex energies  $E$ . For time independent vorticities  $\omega$ , the vortex radius  $R$  is obtained from its energy from the relation  $E \approx \omega^2 R^4$ . The strategy is to characterise the vortex energy population  $\Phi(E, t)$  by the moments  $m_\alpha = \int_0^\infty l^\alpha \phi(l) dl$ , where we use the scaling ansatz of the vortex energy/size distribution

$$\Phi(E, t) = \frac{1}{\epsilon^2} \phi\left(\frac{E}{\epsilon}\right) , \quad (19)$$

and  $\epsilon(t)$  is the characteristic (time-dependent) vortex energy. The exponent  $-2$  is required by (approximate) energy conservation. Note that calculating a moment corresponds to taking the Mellin transform of  $\phi(l)$ . This implies that if we know  $m_\alpha$ , we are able to retrieve  $\phi(l)$  by taking the inverse Mellin transform.

Adapting from Cheng and Redner [24], we obtain the equations of evolution for the vortex size population. Assuming that the fusion rate between two vortices of similar energy  $E$  is a power law  $E^\beta$  and calling  $b(x)$  the probability that the ratio between the final vortex energy and each of the initial fusing vortex be  $x$ , we substitute the scaling ansatz (19) in the linear Smoluchowsky aggregation equations and obtain two separate equations with a separation constant  $\omega$ , one for the time dependence of  $\epsilon(t)$  and the other for the scaling function  $\phi$ . In terms of the moments  $m_\alpha$  of  $\phi$ , we get the following recurrence equations :

$$m_{\alpha+\beta} = \omega \frac{1-\alpha}{L_\alpha-1} m_\alpha , \quad (20)$$

and

$$L_\alpha = \int_0^1 x^\alpha b(x) dx , \quad (21)$$

From the term  $\frac{1}{L_\alpha-1}$  in (20), we see that if there exist a value  $\alpha^*$  such that

$$L_{\alpha^*} = 1 , \quad (22)$$

then all moments with  $\alpha > \alpha^*$  will become infinite. Provided reasonable analyticity conditions hold, it follows that the value  $\alpha^*$  is a pole of  $m_\alpha$ . Taking the inverse Mellin transform of  $m_\alpha$  then allows us to get  $\phi(l)$  and, using the existence of the pole at  $\alpha^*$ , this immediately predict that

$$\phi(l) \sim l^{-(1+\beta+\alpha^*)} , \quad (23)$$

One can check that for a large variety of  $b(x)$ , there are solutions of (22) with complex exponents  $\alpha^*$ . This signals the existence of log-periodic corrections to a pure power law distribution of vortex sizes. Such a scenario has been documented experimentally in the reverse situation of fragmentation in Ref.[25]. This, in turn, leads to a complex separation constant  $\omega$ , and thus to a complex dynamical exponent  $\xi$  for the time evolution.

### 3 Methodology of the data analysis

Detecting log-periodic structures in noisy, intermittent data is rather subtle and apparently innocent data manipulations, such as using the cumulative distribution rather than the data itself, may completely erase such structures. Furthermore, since these structures are *log*-periodic it is often impossible to obtain a large number of oscillations, since numerical and experimental data seldom cover more than a few decades. Hence, great care must be taken not only with respect to what quantity to analyse in an attempt to quantify the strength and frequency of a log-periodic signal but also how to average different realisations. Here the question of noise also enters crucially, since the higher the noise level the more oscillations are necessary. The next section will try to shed light on these technical questions and provide guidelines for the analysis of the turbulent data.

If we suspect that some distribution  $p(x)$  obeys

$$p(x) \propto x^\alpha \quad (24)$$

and furthermore believe  $\alpha$  to be complex, the most direct quantification is to look at the logarithmic derivative

$$\frac{d \ln p(x)}{d \ln x} = \alpha. \quad (25)$$

There are a number of ways to estimate the derivative from data, but they more or less amount to the same thing, namely locally estimating the data by some function, typically a

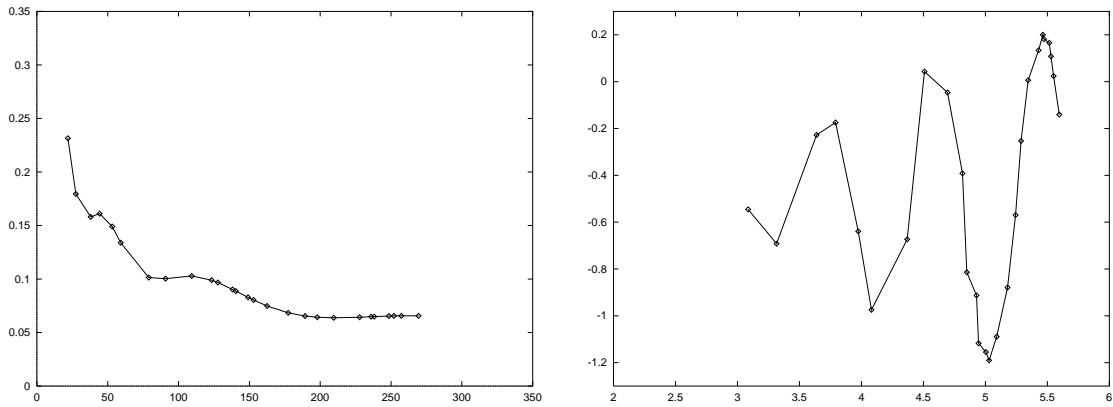


Figure 1: First synthetic data set and it's logarithmic derivative.

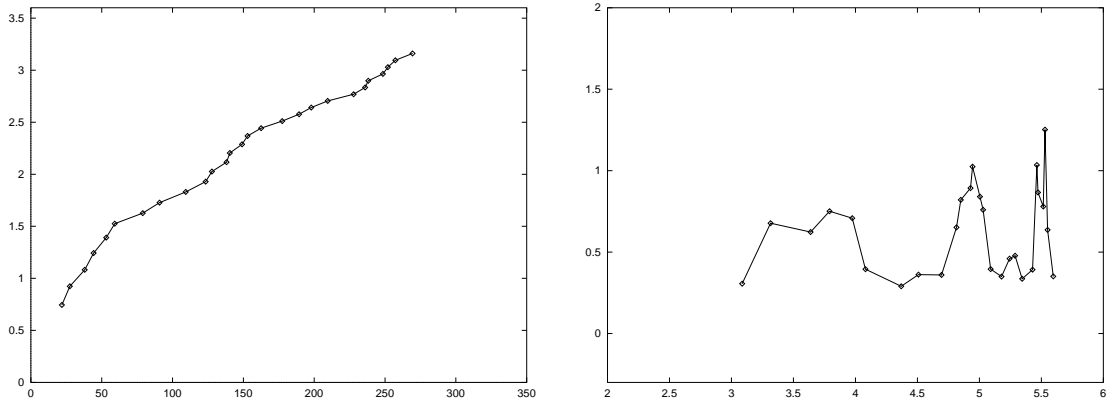


Figure 2: The cumulative distributions of the data set in figure 1 and it's logarithmic derivative.

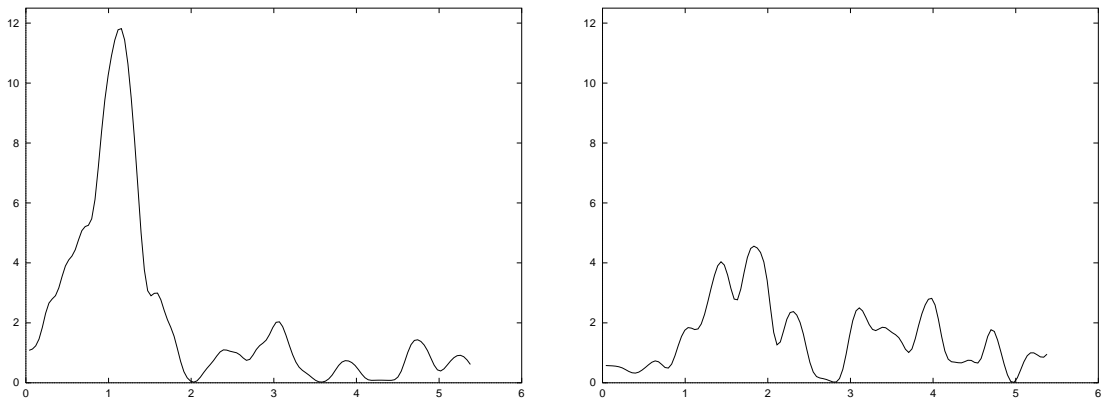


Figure 3: Lomb periodograms of the derivatives in figures 1 (left) and 2 (right).



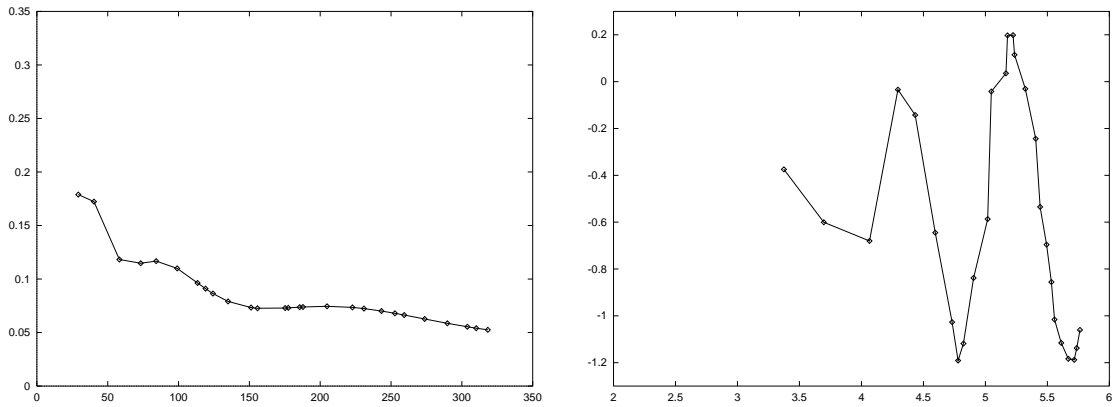


Figure 4: Second synthetic data set and it's logarithmic derivative.

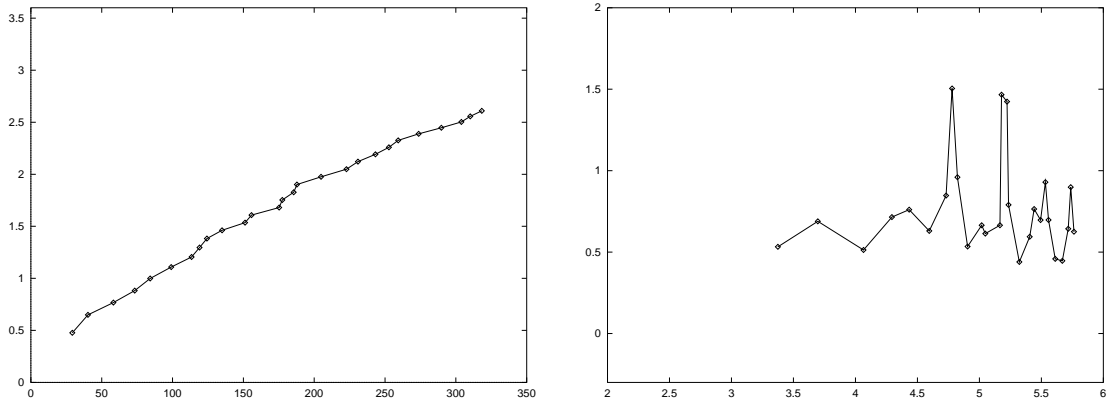


Figure 5: The cumulative distributions of the data set in figure 4 and it's logarithmic derivative.

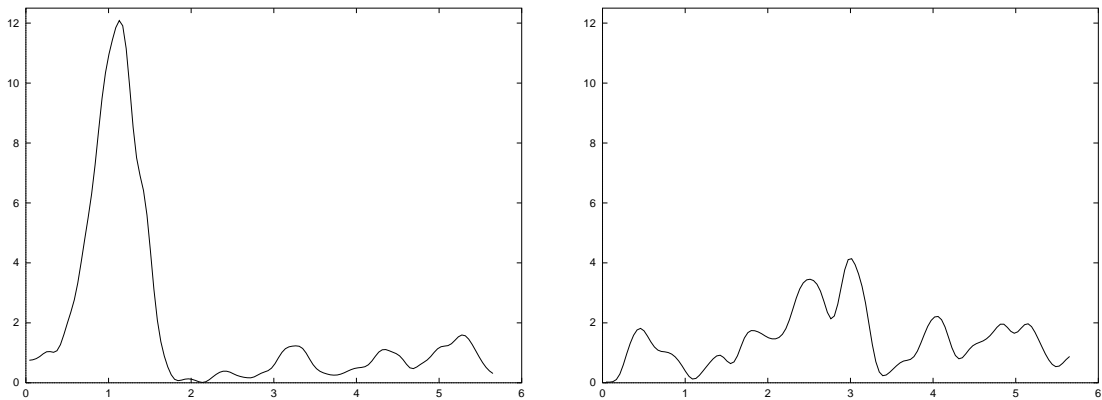


Figure 6: Lomb periodograms of the derivatives in figures 4 (left) and 5 (right).

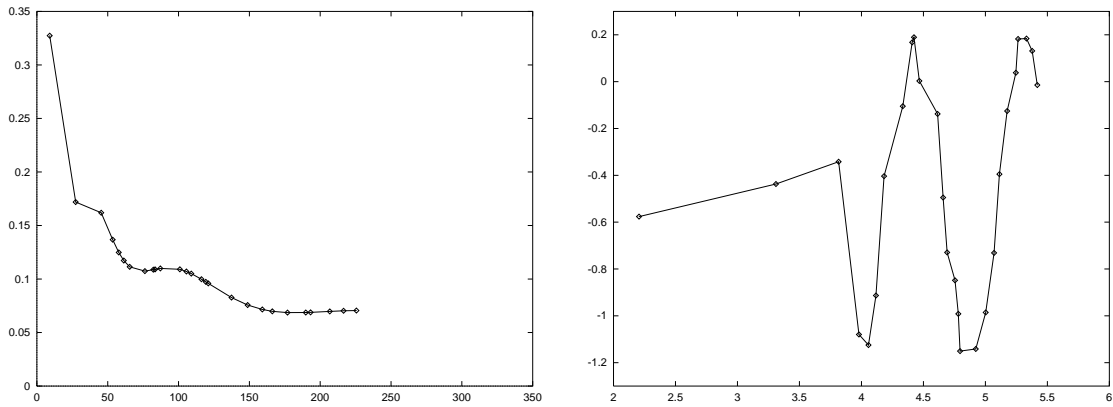


Figure 7: Third synthetic data set and it's logarithmic derivative.

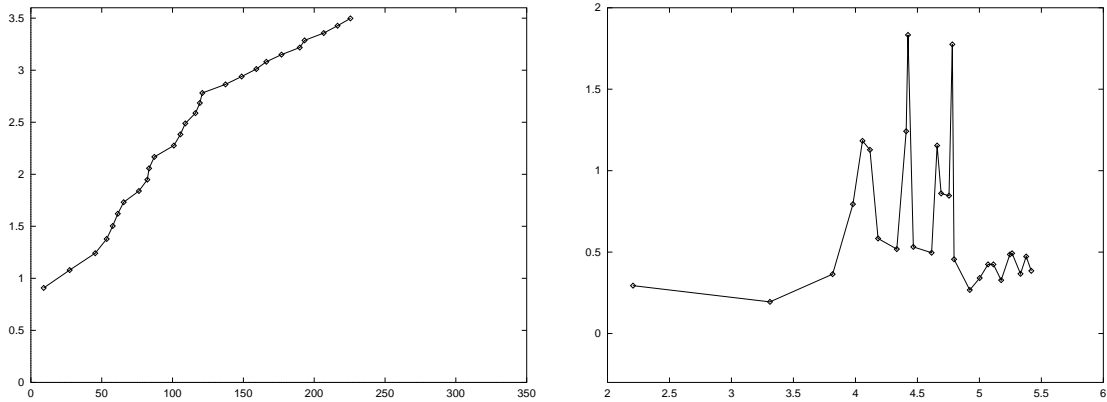


Figure 8: The cumulative distributions of the data set in figure 7 and it's logarithmic derivative.

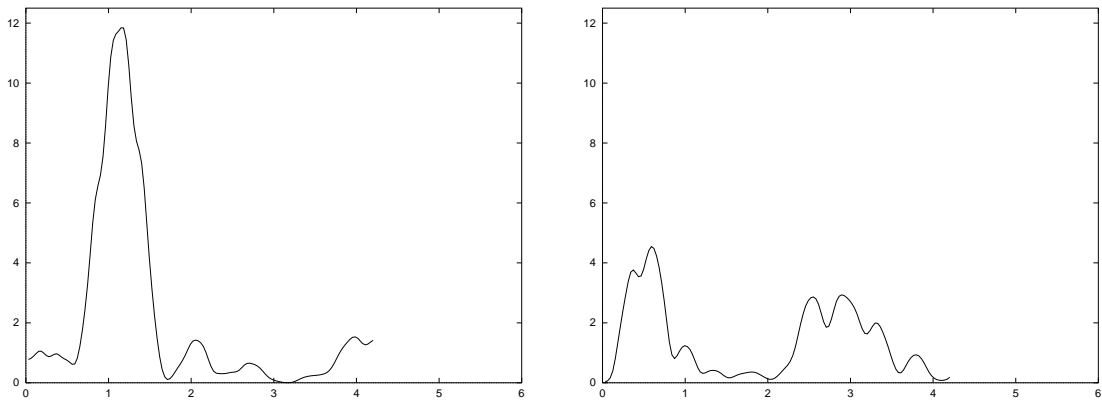


Figure 9: Lomb periodograms of the derivatives in figures 7 (left) and 8 (right).

nth degree polynomial and then performing the derivative. Performing the derivative directly on discrete data amounts to drawing a line between consecutive data points and using its slope as the derivative. A more sophisticated Savitsky-Golav filter [26] uses polynomials of arbitrary degree and preserves higher moments of the data, such as the variance, which becomes suppressed with a moving average (hence, a moving average is unsuitable in an analysis for log-periodicity). However, in the following we will use the simplest numerical procedure to calculate the derivative, i.e.,

$$\left. \frac{d \ln p(x)}{d \ln x} \right|_{x=x_i} = \frac{\ln p(x_{i+1}) - \ln p(x_{i-1})}{\ln x_{i+1} - \ln x_{i-1}} \quad (26)$$

in order to keep the numerical manipulation transparent.

A numerical tool that we will use extensively in this paper is the so-called Lomb periodogram [26]. It corresponds to a harmonic analysis using a series of local fits of a cosine (with a phase) with some user chosen range of frequencies. The advantage of the Lomb periodogram over a Fast Fourier transform is that the points does not have to be equidistantly sampled, which is the case here.

### 3.1 The Lomb periodogram and integration

A method often used in order to investigate fluctuations in data is to fit the average behaviour of the data by some function which is then subtracted. This method can be justified if you *only* want to estimate the error of that specific fit. However, you cannot use it to extract oscillations unless you have many and if that's the case you can do much better with the data itself. The problem with the procedure is that the somewhat arbitrary "truncation" of the data set in both ends will produce a bias due to the randomness of the phases of each realisation. If some sort of de-trending is to be used in order to accentuate the more subtle correlations, such as log-periodicity, then it always makes more sense to *divide* the data by the leading trend rather than subtracting it. However, it's a non-trivial task to get an un-biased estimate of such a leading trend due to the same arbitrary truncation. When this is possible, such a de-trending is a very powerful way of visualising log-periodic oscillations. This has been clearly illustrated in the case of financial data [27].

Another troublesome feature of extracting log-periodic components from data is that they can easily be destroyed by "innocent" data manipulation such as calculating the cumulative distribution. An example where this is clearly the case is shown below. We have generated 10 data sets with 30 points each using the equation

$$y(t) = t^{-0.5} [1 + 0.1 \cdot \cos(2\pi f \ln t)] \quad \text{with } f = 1.114 \quad (27)$$

where the sampling was random in the sense that the spacing between two consecutive points was chosen from the interval  $[0 : 20]$  with uniform probability.

Figures (1,4,7) show three typical realizations of the random sampling of (27) together with the corresponding discrete estimations of their logarithmic derivatives. Figures (2,5,8) show the corresponding integrals (cumulatives) of the three samples together with the discrete estimations of their logarithmic derivatives. Figures (3,6,9) compare the Lomb spectrum of the direct and cumulative sampling presented in the previous figures. Whereas we clearly extract the log-periodic component in the signal and its frequency  $f = 1.1$  with a level of significance better than 0.995 (see Ref.[26] for the quantification of the significance from the peak level), the signal has completely disappeared in the cumulative distribution.

This not only shows that a relatively strong (10% in amplitude) log-periodic signal will be destroyed by an seemingly innocent summation but also that without noise only  $\approx 2$  oscillations is enough to qualify log-periodicity. Similarly to the performance of a FFT which depends on

the ratio of the measured frequency over the Nyquist frequency as well as the length of the time series, the performance of the Lomb periodogram depends on the number of points per oscillation and the number of oscillations. In fact, this example confirms very well the general belief that noise in data can be “integrated out” and that constructing cumulatives provides a very efficient low-pass ( $1/f^2$ ) filter. However, for our present task of identifying log-periodicity, it also shows the danger of this procedure which integrates out both the noise and the useful signal.

### 3.2 Additive noise

The process used in generating figures (1,4,7) is already noisy in some sense due to the random sampling.\* We now investigate the effect of additive noise, in addition to the irregular sampling. We have thus added a noise term to equation (27) and rewritten it as

$$y(t) = (1 + k(0.5 - ran))t^{-0.5} [1 + 0.1 \cdot \cos(2\pi f \ln t)] , \quad \text{with } f = 1.114 , \quad (28)$$

where  $k$  is the amplitude of the noise and  $ran$  is the intrinsic random number generator of Fortran. In figures 10 to 12 we see 3 examples of such synthetic data sets and their corresponding Lomb periodograms. Here  $k = 0.1$  is used corresponding to a noise level half of the amplitude of the log-periodic oscillations. What we see now is that the confidence interval has come down considerable, but the peak is still correctly positioned for all 10 data sets of which 3 arbitrary sets are shown here. In fact, what we see here is not very much different from the analysis of diffusion limited aggregation (DLA) presented in [28, 29]. The individual data set do not carry a very large significance, but the consistence of the analysis for the entire ensemble of data sets do.

If we increase the noise by a factor of 2, *i.e.*, to the same amplitude as that of the log-periodic oscillation things become very murky, but it is still possible to identify the log-periodic oscillations using the results for the entire *ensemble*. If we, as for DLA [28, 29], record the two highest peaks for the 10 data sets, we get the distribution shown in figure 13. It is rather remarkably that, with the Lomb periodogram, we can retrieve log-periodicity with such quality in data which has a noise amplitude of the same size as that of the log-periodicity. In the next section, we shall see a more elegant way of retrieving log-periodicity in noisy data.

### 3.3 The method of canonical averaging

The method of “canonical averaging” has been introduced [30] to reveal subtle correlations which would disappear in the usual ensemble averaging. We have tested a specific implementation of it on log-periodicity in DLA clusters and rupture time-to-failure processes [28, 29, 31], based on a sample-dependent phase determined from the maximum of a sample-dependent susceptibility.

Recall that the problem comes from the fact that the argument  $2\pi f \ln t$  in the cosine in equation (27) is defined up to a phase, since adding a phase simply corresponds to a change of time units. In other words, the universal physical quantity is the log-frequency  $f$  while the phase is expected to be sample-specific and to fluctuate from realizations to realizations [31]. If this problem is not addressed properly, standard averaging procedure mix measurements with different phases leading to a destructive interference of the log-periodic oscillations.

We now propose a much simpler method than previously used [31] whose principle is to “re-phase” the oscillations. The method is based on the fact that a Lomb periodogram is a simple

---

\*It is probably better to keep the vocable “noise” for processes that deteriorate the signal. In the case of a random sampling of  $n$  points in some interval  $T$ , frequency components which are larger than the Nyquist frequency of the corresponding evenly sampled points  $\frac{N}{2T}$  can be identified. Hence, the random sampling is in fact improving the signal-to-noise ratio for high frequencies.

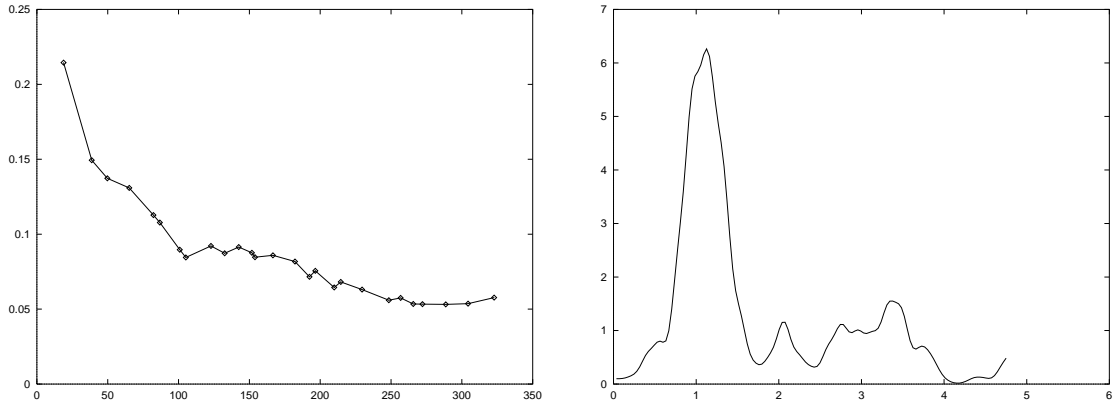


Figure 10: First noisy data set (left) and Lomb periodogram of its logarithmic derivative (right).

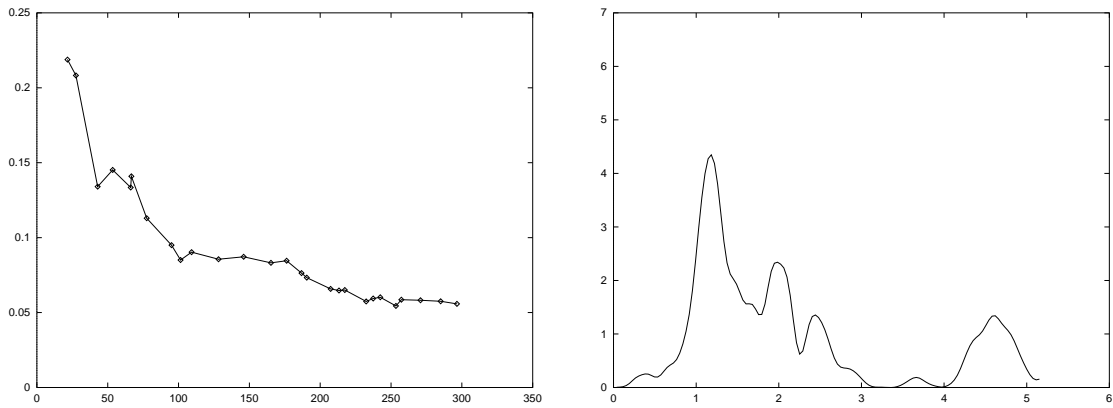


Figure 11: Second noisy data set (left) and Lomb periodogram of its logarithmic derivative (right).

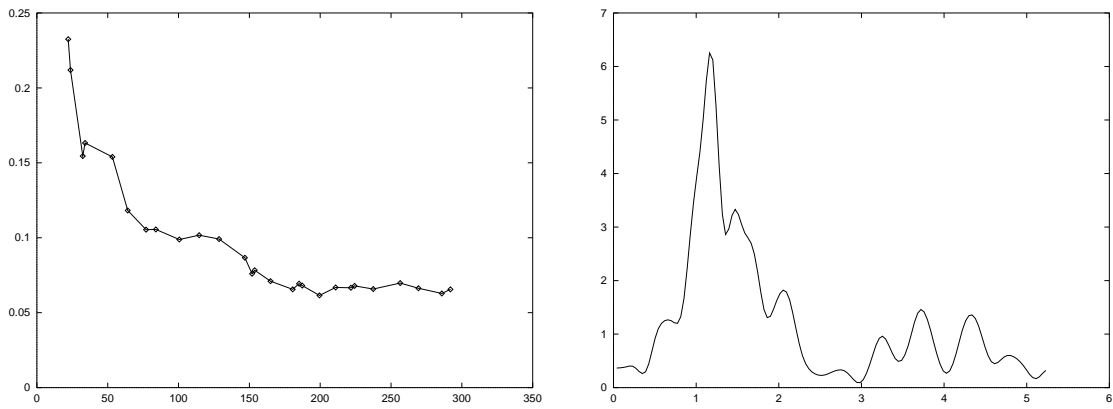


Figure 12: Third noisy data set(left) and Lomb periodogram of its logarithmic derivative (right).

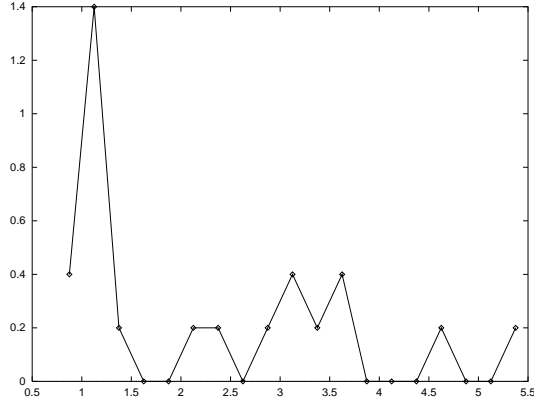


Figure 13: Histogram of the frequency distribution for the two most significant peaks in the Lomb periodogram of 10 data sets with a noise amplitude of the same size as the amplitude of the log-periodic oscillations. The peak in the histogram correspond to a frequency of  $\approx 1.12$  in very good agreement with that of  $f \approx 1.114$  used.

cosine fit, while the phase is not playing any role. Hence, the periodogram corresponds to a removal of the phase from the data. This means that averaging the periodograms of different data sets is exactly the “re-phasing” we are looking for. In figure 14, we show the averaged periodogram for the 10 data sets used in the histogram shown in figure 13. The two peaks corresponds two frequencies of and 1.13 and 3.4, respectively. The first and most significant peak is in very good agreement with the frequency of 1.114 used in generating the data sets. The second peak is furthermore in excellent agreement with that of the third harmonic. We remind the reader that figure 14 comes from averaging periodograms of noisy data with a noise-amplitude of the *same size* as the amplitude of the log-periodic oscillations. Nevertheless, the log-frequency component of  $\approx 1.1$  present in the data is unambiguously extracted as well as its third harmonic hardly visible in the histogram in figure 13. This illustrates not only the efficiency of the Lomb periodogram in retrieving periodic trends, but also that of the canonical averaging scheme for re-phasing the oscillations.

This concludes the numerical tests of the tools to be used in the experimental data analysis that we present in the next section.

## 4 Experiments on 2-d freely decaying turbulence

The experimental data analysed here are some of those presented in [22] (Fig.’s 6 and 7). We will briefly describe the experimental techniques and the results that are used in the present context.

### 4.1 Experimental setup

The flow is generated in a thin, density stratified layer of electrolyte, using an electro-magnetic forcing. During a short initial forcing period, an  $8 \times 8$  array of vortices is created, with nearest neighbours counter-rotating. At a time defined as  $t = 0$ , the forcing is stopped, and the system is then decaying freely. After a vertical reorganisation of the flow with a maximum duration of 2 seconds, the system can be regarded as two-dimensional, except for the effect of bottom friction [32], which causes an exponential decay of the total energy of the system with a well-defined

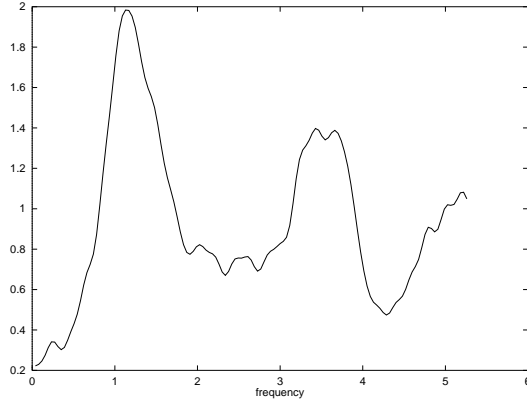


Figure 14: The averaged Lomb periodograms of the 10 data sets used in the histogram shown in figure 13. We emphasise that the amplitude of the noise was of the same size as the amplitude of the log-periodic oscillations. Note that the true confidence interval does not correspond to the values shown, since it’s an average over 10 data sets. The value of the two peaks are 1.13 and 3.4 and in excellent agreement with the 1. and 3. harmonic of the frequency  $f \approx 1.114$  used in generating the data sets.

time constant. A rescaling of time is applied under which we can consider the system as truly two-dimensional [22].

The size of the experimental system is  $15 \text{ cm} \times 15 \text{ cm}$ , and the initial Reynolds number is typically 1800. The duration of the experiments is approximately 12 seconds in rescaled time units.

## 4.2 Determination of vortex statistics

The velocity field  $\mathbf{v}(x, y)$  on the free surface of the fluid is determined using the Particle Image Velocimetry (PIV) technique described in [33], with a resolution of  $40 \times 40$  measurement points. From the velocity field, the vorticity field  $\omega(x, y) = \partial_x v_y - \partial_y v_x$  is computed using a polynomial fit. Typically 70 velocity fields are calculated during the time of the experiment. The vorticity field is analysed for vortices by searching for local extrema with the absolute vorticity above a threshold. The results are not sensitive to the choice of threshold, and the recognition method has been checked with other methods. Thus we can define a number  $n$  of vortices for each velocity field. The position of a vortex is defined as the position of the vorticity extremum. This is used to extract the mean nearest-neighbour separation  $r$  of the vortices. The size of a vortex is defined by the connected area with an absolute vorticity above the threshold. For each velocity field the mean vortex radius  $a$  is computed from the mean vortex size.

## 4.3 Scaling laws

Rapidly after the forcing has been stopped, like-sign vortices start to merge. Fewer and larger structures are thus formed, and this continues until the energy of the system is so small that no further evolution of the vortices can be observed.

We presented [22] measurements that are averages of 9 experimental realizations (in the case of vortex radius, only 7 realizations were used). We found that for the time period from  $t = 1.5$

s to  $t = 10$  s the quantities defined above follow the power laws

$$\begin{aligned} n(t) &\sim t^{-0.70\pm 0.1} \\ a(t) &\sim t^{0.21\pm 0.06} \\ r(t) &\sim t^{0.38\pm 0.08}. \end{aligned} \tag{29}$$

The error bars are estimated by considering the fluctuations observed between individual realizations, *however* without any re-phasing of the log-periodic oscillations to be extracted in section 4.4. We note that the average values for the exponents in (29) agree well with the scaling approach [34].

## 4.4 Log-periodic analysis of the experimental data

As explained in the previous section, three experimentally independent quantities has been measured as a function of time: the number of vortices,  $n(t)$ , the mean vortex radius  $a(t)$  and the mean distance between vortices  $r(t)$ . For each of these quantities, the log-periodic signatures present in the data will be extracted using the tools described in the section 3. Specifically, the logarithmic derivative as defined by eq. 25 was calculated from the experimental data. Truncating the times series in order to avoid end-effects gave  $\approx 35$  points for each periodogram to use. This corresponds well to the 30 points used in the synthetic data analysis of section 3.

### 4.4.1 Number of vortices

In figure 15, we see the number of vortices  $n(t)$  as a function of re-scaled time  $t$  (left) and its logarithmic derivative (right) for a specific experimental realisation. In figure 16 (left), we see the corresponding periodogram of the logarithmic derivative shown in figure 15 with a peak at a log-frequency of  $\approx 4$ . The height of the peak is only approximately twice the height of the second largest which means that the confidence of the peak is not very high. Nevertheless, performing a simple average of the Lomb periodograms for the 9 available experimental realisations gives us the picture shown in figure 16 (right). The peak has moved up slightly but is still clearly visible, which means that the position of a peak at a frequency of  $\approx 4$  for the single realisation was not accidental, since a pure noise signal would have disappeared in an average over 9 realisations. We stress that a frequency of  $\approx 4$  is approximately a factor 5 below the average sampling frequency of  $1.6/35 \approx 22$ . This means that the number of points per oscillation is smaller than that of the synthetic data which explains the lesser performance.

### 4.4.2 Mean separation of vortices

In figure 17, we see the average separation between vortices  $r(t)$  as a function of re-scaled time  $t$  (left) and its logarithmic derivative (right) for an specific experimental realisation. In figure 18 (left), we again see the corresponding periodogram of the logarithmic derivative shown in figure 17 with a peak at a frequency of  $\approx 4$ . The height of the peak is again only approximately twice the height of the second largest. Nevertheless, performing the average of the Lomb periodograms for 9 experimental realisations gives us the picture shown in figure 18 (right). The peak has again moved up slightly but is still clearly visible, which again means that the position of a peak at a frequency of  $\approx 4$  for the single realisation was not accidental.

### 4.4.3 Mean radius of vortices

In figure 19, we see the mean radius of the vortices  $a(t)$  as a function of re-scaled time  $t$  (left) and its logarithmic derivative (right) for an specific experimental realisation. In figure 20 (left), we



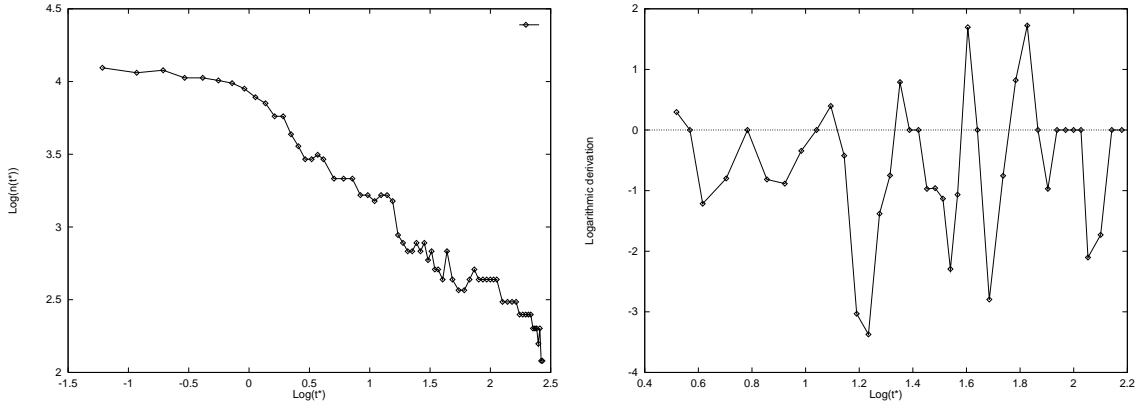


Figure 15: Logarithm of the number of vortices  $\log(n(t))$  as a function of the logarithm of re-scaled time  $\log(t)$  (left). The corresponding logarithmic derivative as a function of  $\log(t)$  (right).

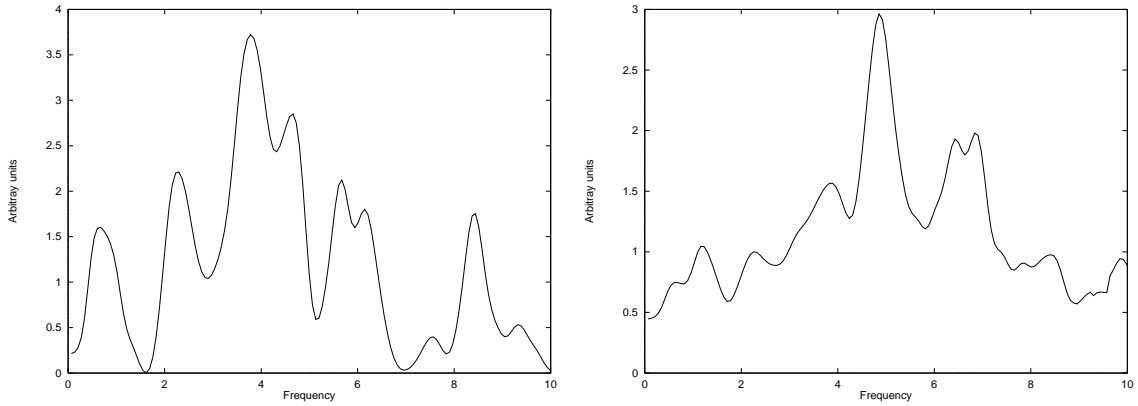


Figure 16: Lomb periodogram of the logarithmic derivative shown in figure 15 (left). Lomb periodogram of the logarithmic derivative of the number of vortices  $n(t)$  as a function of re-scaled time  $t$  averaged over 9 experimental realisations (right).

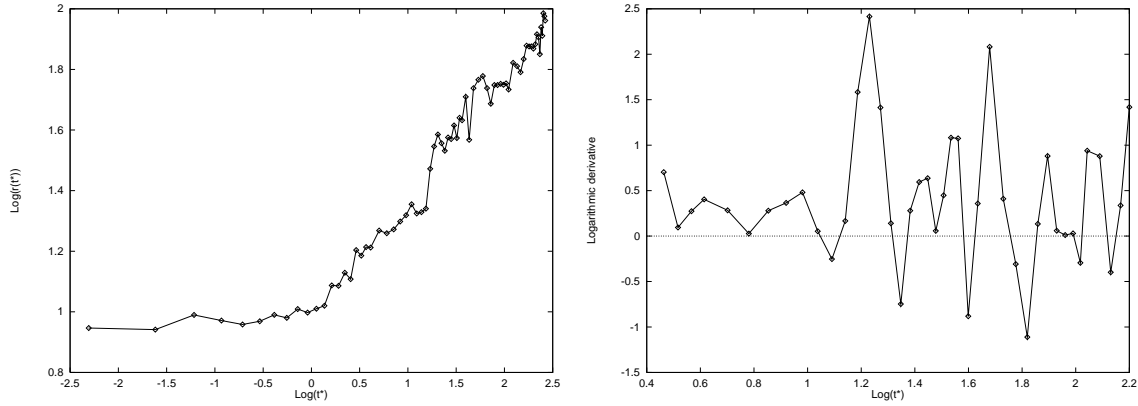


Figure 17: Logarithm of the mean separation of vortices  $\log(r(t))$  as a function of the logarithm of re-scaled time  $\log(t)$  (left). The corresponding logarithmic derivative as a function of  $\log(t)$  (right).

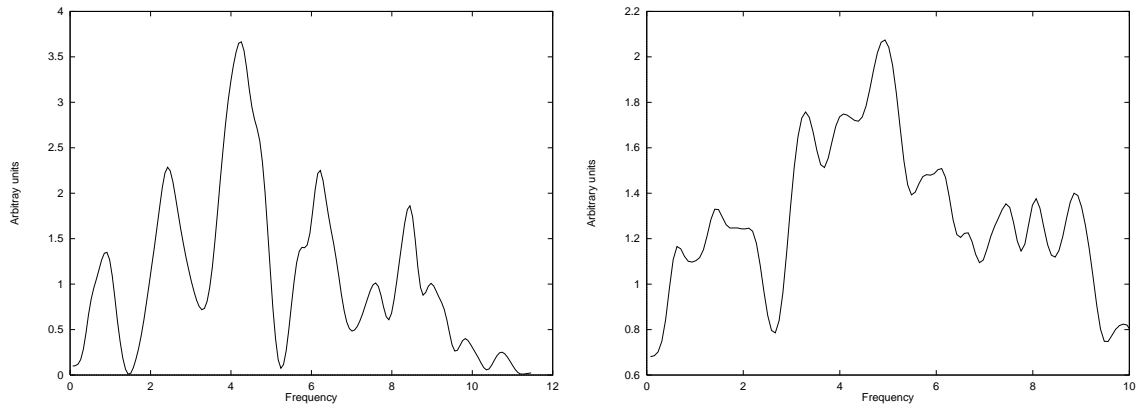


Figure 18: Lomb periodogram of the logarithmic derivative shown in figure 17 (left). Lomb periodogram of the logarithmic derivative of the mean separation of vortices  $r(t)$  as a function of re-scaled time  $t$  averaged over 9 experimental realisations (right).

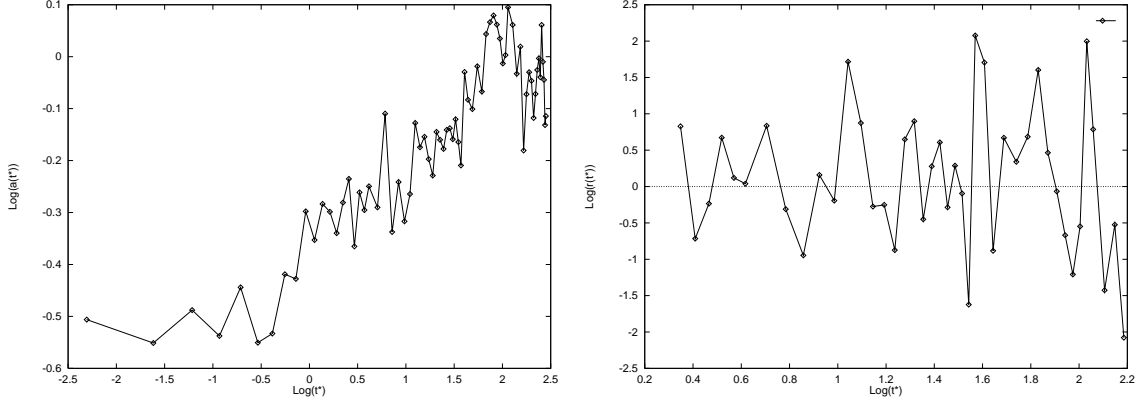


Figure 19: Logarithm of the mean radius of the vortices  $\log(a(t))$  as a function of the logarithm of re-scaled time  $\log(t)$  (left). The corresponding logarithmic derivative as a function of  $\log(t)$ .

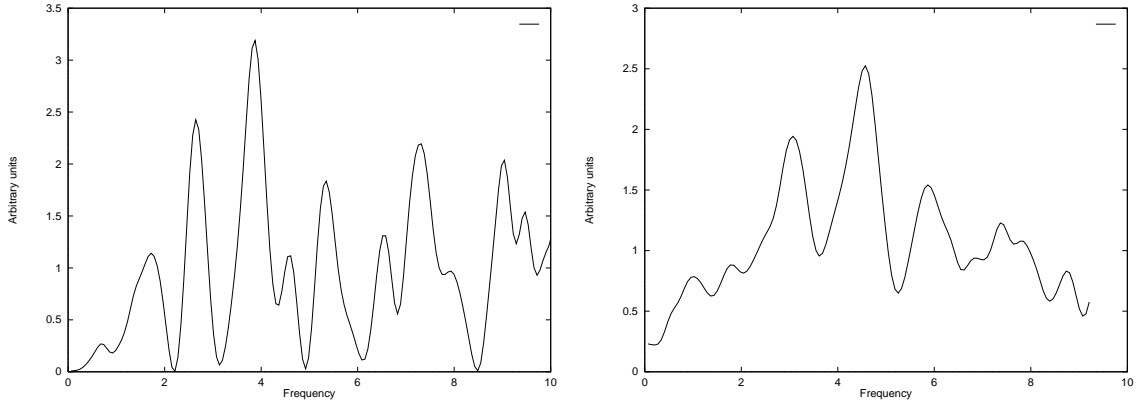


Figure 20: Lomb periodogram of the logarithmic derivative shown in figure 19 (left). Lomb periodogram of the logarithmic derivative of the mean radius of the vortices  $a(t)$  as a function of re-scaled time  $t$  averaged over 7 experimental realisations (right).

see the corresponding periodogram of the logarithmic derivative shown in figure 19 with a peak at a (log-) frequency of  $\approx 4$ . The height of the peak is again only approximately twice the height of the second largest. Performing the average of the Lomb periodograms for 7 experimental realisations available here gives us the picture shown in figure 20 (right). The peak is rather broad but is still clearly visible, which again signifies that the position of a peak at a frequency of  $\approx 4$  for the single realisation was not accidental.

## 5 Conclusion

We have suggested that the concept of *discrete* time scale invariance of the underlying physics is more appropriate for the description of freely decaying 2-d turbulence than the usual assumption of a continuous time scale invariance.

In this goal, a numerical analysis of synthetic data have demonstrated a new canonical averaging scheme using the Lomb periodogram as its main ingredient. We have furthermore

shown that seemingly innocent data manipulations completely destroy the log-periodic structures in these synthetic data.

Using this new canonical averaging scheme on experimental data obtained from freely decaying 2-d turbulence, we have shown that the log-periodic signatures slightly visible in the individual experimental realisations carry statistical significance and cannot be disregarded as noise when averaged over the nine available experimental realizations. It is quite reassuring that the analysis of the three different experimentally independent measurements all agree on a log-frequency of  $\approx 4 - 5$  for the identified log-periodic oscillations. This correspond to a preferred scale factor  $\lambda \equiv e^{1/f} \approx 1.2 - 1.3$

Our study of this experiment establishes for the first time a systematic procedure for exploring the existence of log-periodic oscillations in turbulence data. In this spirit, it would be very interesting to analyse previous partial indications of log-periodicity in turbulent data, that can be found in fig. 5.1 p.58 and fig. 8.6 p.128 of Ref. [1], fig.3.16 p. 76 of Ref.[35], fig.1b of Ref.[36] and fig. 2b of Ref. [37].

For a theoretical view point, we have presented a theoretical framework which makes plausible the presence of log-periodic oscillations in the observables. Physically, we interpret the observed log-periodicity as resulting from a discrete cascade of intermittent vortex coalescence processes. In this sense, 2-d freely decaying turbulence would not be much different from other systems in which log-periodicity has been documented to result from self-similar intermittent instabilities [5].

From the point of view of the Navier-Stokes equations, it may seem remarkable or even stretching credibility that log-periodicity emerges from such continuous PDE. A possible analogy is offered by the recent discovery that the continuous nonlinear Einstein PDE's of general relativity in the presence of a scalar field self-interacting through gravitation may generate a log-periodic spectrum of black hole masses with develop according to a log-periodic self-similar time dynamics [38]. The mechanism might result from the existence of a limit cycle in the renormalisation group description of a field close to the negative density limit (in turbulence, could this be obtained from a negative effective viscosity?). Another possible route [13] is that scale invariant equations that present an instability at finite wave-vector  $k$  decreasing with the field amplitude may generate naturally a self-similar discrete spectrum of internal scales.

We acknowledge useful comments from A. Arnéodo, B. Dubrulle, U. Frisch and P. Tabeling.

## References

- [1] Frisch, U. (1995) *Turbulence, the legacy of A.N. Kolmogorov*, Cambridge University Press.
- [2] R.H. Kraichnan, Phys. Fluids **10**, 1417 (1967)
- [3] Z.-S. She, Hierarchical structures and scalings in turbulence, Lecture Notes in Physics, eds. Eden *et al.* (1997); Universal laws of cascade of turbulent fluctuations, in Proceedings of the 12th Nishinomiya Symposium (1998).
- [4] J. Paret and P. Tabeling, Phys. Fluids **10n** 3126 (1998)
- [5] D. Sornette, Phys. Reports 297, 239 (1998). (see <http://xxx.lanl.gov/abs/cond-mat/9707012> for an extended version)
- [6] H. Saleur and D. Sornette, J. Phys. I France 6, 327 (1996)
- [7] J.C. McWilliams, J. Fluid Mech. **146**, 21 (1984)
- [8] Barenblatt, G. I. (1996) *Scaling, self-similarity, and intermediate asymptotics*, Cambridge University Press.
- [9] G.K. Batchelor, Phys. Fluids Suppl. II 12, 233 (1969)
- [10] Barenblatt, G.I. & Goldenfeld, N. (1995) *Phys. Fluids* **7**, pp. 3078-3082.
- [11] B. Dubrulle, (1996) *J. Phys. France II* **6**, pp. 1825-1840.
- [12] B. Dubrulle, Scale Invariance and Statistical Properties of Turbulence, Thèse d'habilitation à diriger des recherches, Université de Paris 7 (1996)
- [13] D. Sornette, Discrete scale invariance in turbulence? in the Proceedings of the Seventh European Turbulence Conference (ETC-7), June 30-July 3 (1998) (Published by Kluwer, U. Frisch, editor) (<http://xxx.lanl.gov/abs/cond-mat/9802121>)
- [14] Novikov, E.A. (1966) *Dokl.Akad.Nauk SSSR* **168/6**, pp. 1279; (1990) *Phys.Fluids A* **2**, pp. 814-820.
- [15] Anselmet, F., Gagne, Y., Hopfinger, E.J. & Antonia, R.A. (1984) *J. Fluid Mech.* **140**, pp. 63
- [16] E. Trizac, Europhys. Lett. 43, 671 (1998)
- [17] Y. Pomeau, J. Plasma Physics 56, 407 (1996)
- [18] C. Sire, J. Techn. Phys. 37, 563 (1996) (cond-mat/9503161)
- [19] R. Benzi, S. Patarnello and P. Santangelo, J. Phys. A 21, 1221 (1988)
- [20] J.C. McWilliams, J. Fluid Mech. 219, 361 (1990)
- [21] P.G.J. Van Dongen and M. Ernst, J. Stat. Phys. 50, 295 (1988)
- [22] A.E. Hansen, D. Marteau and P. Tabeling, Phys. Rev. E 58, 7261 (1998)
- [23] Redner, S., Fragmentation, in *Statistical models for the fracture of disordered media*, H.J. Herrmann and S. Roux editors, Elsevier Science Publishers, 1990

- [24] Cheng, Z., and S. Redner, Phys.Rev.Lett. 60, 2450 (1988).
- [25] G. Ouillon, D. Sornette, A. Genter and C. Castaing, J. Phys. I France 6, 1127 (1996)
- [26] W.H. Press, B.P. Flannery, S.A. Teukolsky and W.T. Vetterling, Numerical Recipes (Cambridge University Press, Cambridge UK, 1992).
- [27] A. Johansen and D. Sornette, RISK 12 (1), 91 (1999) (<http://xxx.lanl.gov/abs/cond-mat/9901035>).
- [28] D. Sornette, A. Johansen A. Arneodo, J.-F. Muzy and H. Saleur, Phys. Rev. Lett. 76, 251 (1996)
- [29] A. Johansen, Discrete scale invariance and other cooperative phenomena in spatially extended systems with threshold dynamics, Ph.D. Thesis, Niels Bohr Inst. (Dec. 1997). Available on [www.nbi.dk/~johansen/pub.html](http://www.nbi.dk/~johansen/pub.html)
- [30] F. Pazmandi, R.T. Scalettar and G.T. Zimanyi, Phys. Rev. Lett. 79, 5130 (1997)
- [31] A. Johansen and D.Sornette, Int. J. Mod. Phys. C9 (3), 433 (1998)
- [32] J. Paret, D. Marteau, O. Paireau, P. Tabeling, Phys. Fluids 9 (10), 2752 (1997)
- [33] O. Cardoso, D. Marteau, P. Tabeling, Phys. Rev. E 49, 454 (1994)
- [34] G.F. Carnevale, J.C. McWilliams, Y. Pomeau, J.B. Weiss and W.R. Young, Phys. Rev. Lett. 66, 2735 (1991)
- [35] A. Arnéodo, Argoul, F., Bacry, E., Elezgaray, J. & Muzy, J.-F. (1995) *Ondelettes, multifractales et turbulences*, Diderot Editeur, Arts et Sciences
- [36] Tchéou, J.-M. & Brachet, M.E., J.Phys.II France 6, 937 (1996)
- [37] B. Castaing, in *Scale invariance and beyond*, eds. Dubrulle, B., Graner, F. & Sornette, D., EDP Sciences and Springer, pp. 225–234 (1997)
- [38] M.W. Choptuik, Phys. Rev. Lett. 70, 9 (1993)